Eco. Env. & Cons. 30 (July Suppl. Issue) : 2024; pp. (S452-S459)
Copyright@ EM International
ISSN 0971–765X

DOI No.: http://doi.org/10.53550/EEC.2024.v30i04s.075

Evaluating the impact of Surface Water Dynamics on Agriculture in the Semi-arid Region - A Case Study of Bundelkhand, India

Pratibha Prakash[1], Swadhina Koley[1], S. Naresh Kumar[1]*, R.C. Harit[1], Bidisha Chakrabarti[1] and Manoj Shrivastava[1]

[1]Division of Environment Science, ICAR-Indian Agricultural Research Institute, New Delhi 110 012, India

(Received 29 December, 2023; Accepted 5 February, 2024)

ABSTRACT

Studies on consistent and repetitive observations of surface water bodies over a vast semi-arid region are limited. Such studies are necessary for monitoring surface water dynamics, especially for the Bundelkhand region, a drought prone area. This study captured the availability of surface water for irrigation of rabi season crops such as wheat, mustard, and peas, which are mainly grown in the Bundelkhand region with irrigation. Landsat 8 images were used in this study to estimate the surface water area. The satellite imagery was processed on the cloud-based Google Earth Engine platform. The changes in land use and land cover in the Bundelkhand region for the rabi season were analyzed for 2013-2021 period. This temporal analysis identified patterns and trends in the agriculture, water body, and fallow classes extracted from the Land Use and Land Cover Change (LULC). The Modified Difference Water Index (MNDWI), a multi-band method utilizing spectral differences between two bands, was employed to calculate surface water area. The study concludes that during 2013 to 2021 period, the agricultural area expanded by over 25% and a substantial more than 50% decrease in fallow land during the rabi season. This indicated that increased water availability during winter season has caused an increase in cultivated area during rabi season in Bundelkhand region.

Key words: *Bundelkhand region, Google Earth Engine, Landsat 8, Modified normalized difference Index, Surface water area, Cultivated area.*

Introduction

Surface water constitutes the water bodies above the Earth's surface, including rivers, streams, wetlands, lakes and reservoirs. This critical component of the hydrological cycle serves as a primary and readily accessible water source for human populations (Geographic, 2019; Pekel *et al*., 2016). Playing a pivotal role in regulating ecosystem services and biogeochemical cycles (Pekel *et al*., 2016), surface water is a fundamental natural resource crucial for sustaining life, livelihoods and regional development. This significance is particularly pronounced in the Bundelkhand region of India, which is characterized by water scarcity and susceptibility to drought, and the interannual rainfall variability makes the region susceptible to crop failure (Ahmed *et al*., 2019). Given the escalating demands for water in agriculture, industry, domestic usage, and overall socio-economic development within semi-arid regions (Pricope, 2013), effective mapping and monitoring of surface water resources becomes necessary for planning and management.

The temporal dynamics of surface water, including expansion and shrinkage, is influenced by both natural and anthropogenic factors. Thus, it is necessary to monitor spatio-temporal variations in water bodies for making informed land management decisions (Nie *et al.*, 2011; Pekel *et al*., 2016; Huang *et al.,* 2018; Acharya *et al.,* 2019). Furthermore, the climate change scenario characterized by rising temperatures and alterations in rainfall patterns accentuates the need to monitor dynamic water resource changes in semi-arid regions like Bundelkhand. The study region is increasingly facing the climate change driven weather aberrations posing challenges to water availability necessitating a need-based approach to resource management (Wang *et al.,* 2020). In this context, robust and comprehensive monitoring of surface water resources emerges as an indispensable tool for understanding, adapting to, and mitigating the impacts of environmental changes in water-scarce regions.

In recent times, the development of geospatial technologies has significantly improved our ability to map surface water efficiently over large areas. Monitoring changes in surface water over both space and time has become more accessible due to the availability of time series data from satellites to map the same area repeatedly (Yang *et al.,* 2017; Reddy *et al.,* 2020). These datasets can be applied at various scales, from regional to global (Li *et al.,* 2013; Rokni*et al.,* 2014; Feyisa *et al.,* 2014; Tulbure*et al.,* 2016; Yang *et al.*, 2017; Acharya*et al.,* 2018; Rad, *et al*., 2021).

Many studies use a band ratio approach or spectral index method with multispectral bands to map water bodies because they are quick and easy to implement. This approach involves selecting two bands, typically one from the visible region and another from the near-infrared region (Xu, 2006). The Normalized Difference Water Index (NDWI) is a standard water index that distinguishes water from non-water features by suppressing the latter. The NDWI method uses bands with spectral differences for specific objects, such as surface water, helping to highlight the target object while suppressing the background (Domenikiotis *et al.,* 2003; Yang *et al.,* 2017; Wang *et al.,* 2020). While NDWI is popular, it has a drawback as it struggles to suppress built-up land noise efficiently. The Modified NDWI (MNDWI), developed by Xu in 2006, improved upon NDWI by using the Shortwave Infrared (SWIR) band instead of the Near Infrared (NIR) band. This modification enhanced the capability to extract water features and is widely used for mapping surface water (Wang *et al.,* 2020). The SWIR and green band are used in the MNDWI computation, resulting in positive values for water features and negative values for non-water features (Xu, 2006). Observing surface water using MNDWI is beneficial because it reduces the influence of built-up features associated with surface water and enhances the brightness of the water bodies (ArcGIS, 2021).

Objective of this study is to give an insight into the relationship between water availability and the existing cropping pattern and fallow land area during 2013-2021 period. The present study used the MNDWI to map the surface water area and is correlated with the cropped area during the *Rabi* (November-April) season.

Materials and Methods

Study area description

The Bundelkhand region is situated in the north-central part of India. The Indo Gangetic Plain lies in the northern part of the study area, whereas the Vindhyan mountain range lies in the northwest and southern sides. The Bundelkhand region comprises of seven districts of Uttar Pradesh, namely - Jhansi, Jalaun, Lalitpur, Hamirpur, Mahoba, Banda and Chitrakoot and seven districts of Madhya Pradesh, namely- Datia, Niwari, Tikamgarh, Chhatarpur, Damoh, Sagar and Panna (Figure 1). The total geographical area of the Bundelkhand region is 7.08 million hectares(Mha). The Bundelkhand region lies between 23°20' and 26°20' N latitude and 78°20' and 81°40'E longitude with elevation ranging between 250-300m (Gupta *et al.*, 2014). The study area majorly comprises semi-arid and sub-tropical climate and receives rainfall ranging between 848 mm in the Jhansi district in the northern part of the Bundelkhand region to 1197 mm Sagar district in the southern most part of the region (Tewari *et al*., 2018). The region suffers from acute water scarcity for irrigation and drinking purposes. The major crops of the Bundelkhand region are pigeon pea, urd bean, mung bean, sesame, and soybean, which are sown during *Kharif* (June-October) season, whereas wheat, chickpea, field pea, lentil, linseed and mustard during rabi (November-April) season (Kumar *et al*., 2017).

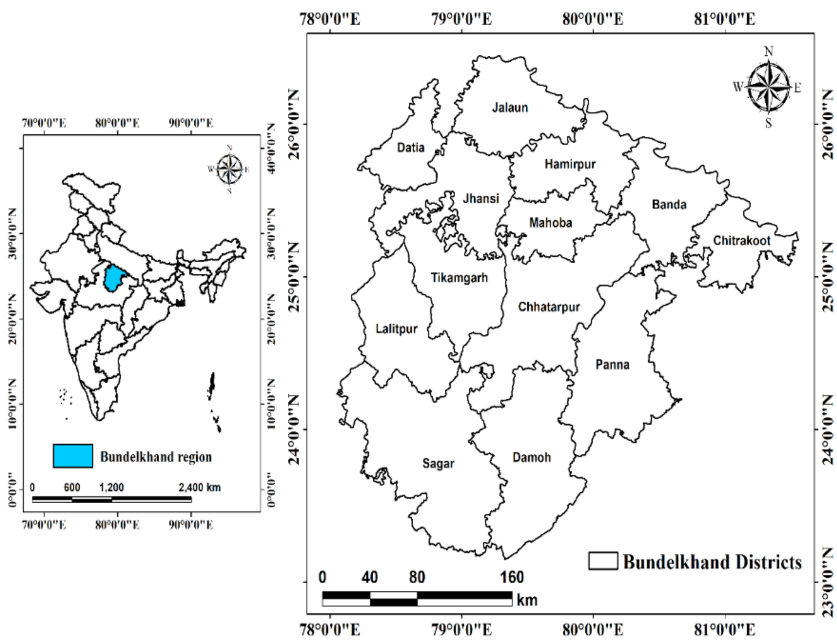

Fig. 1. Map of the study area

Data source

Satellite Data Acquisition

The current study has used the freely available satellite imagery from Landsat 8, a joint venture between the National Aeronautics and Space Administration (NASA) and the U.S. Geological Survey (USGS). The primary advantage of the Landsat series is the availability of long-time series of data at a higher spatial resolution of 30 m with a 16-day repeat cycle. This makes Landsat imagery suitable for mapping surface water due to the availability of medium spatial resolution bands for a longer time duration (Tulbure *et al.*, 2016; Huang *et al.*, 2018). A time series of Landsat 8 surface reflectance imagery was acquired for the post-monsoon (October and November months) season from 2013 to 2021 (Table 1).

JRC dataset

The JRC (Joint Research Centre) Global Surface Water dataset (Table 1) is commonly used for mapping water bodies (Pekel *et al.*, 2016). The JRC dataset typically provides information about the occurrence of surface water over time. The resolution of the JRC monthly water dataset is 30 m. This dataset comprises maps of surface water's location and temporal distribution from 1984 to 2021.

IMD observed gridded data

The rainfall data in millimeters (mm) was derived from the observed daily gridded data provided by the Indian Meteorological Department, which has a high spatial resolution of 0.25 x 0.25 degree (Table 1).

Image preprocessing

The Google Earth Engine (GEE) is an open-source cloud computing platform. It provides easy access to time-series global satellite imagery (Gorelick *et al.*, 2017; Herndon *et al.*, 2020). The GEE platform uses Java Script for computation. The Landsat archive data is on the interactive code editor of GEE, which can be easily assessed for processing. An atmo-

Table 1. Description of the datasets used in the study

Domain	Description	Resolution
Satellite image-based dataset	JRC Global monthly water dataset	30 m
Satellite image-based dataset	Landsat 8	30 m
Gridded dataset	IMD observed gridded data	0.25^{o} x 0.25^{o}

spherically corrected surface reflectance dataset from Landsat imagery was used, and further processing was performed toremove a cloud shadow (Google Earth Engine, 2020).

Image analysis and validation

Land Use Land Cover (LULC)

LULC is a technique to categorize the Earth's surface based on the types and cover present. Land use classes describe the human activities for which the land is being utilized, and land cover refers to the natural features present on the surface of the Earth. Random Forest (RF) Classifier was used for LULC, as it provides high accuracy, fits several decision trees, controls data overfitting and has good predictive accuracy. The code for preparing LULC maps using the random forest algorithm was written in GEE's code editor platform. The LULC classes viz., agriculture, barren land, fallow, forest, urban and water were identified for this study.

Water index calculation

The MNDWI index is computed using the normalized difference between the Green and the mid-infrared (MIR) bands. The advantage of using MNDWI over NDWI is the inclusion of MIR, which is easily absorbed by the water compared to the NIR band used in NDWI. The indices' values range between -1 and +1, where the positive value represents water (0 to 1) and the negative values (-1 to 0) represent non-water features. The soil and vegetation will also have negative values as they reflect MIR more than NIR (Xu, 2006). The threshold value for differentiating water from non-water features can be taken at zero (Xu, 2006). This method is relatively fast for differentiating water and non-water features (Acharya, Subedi and Lee, 2018). The MNDWI is developed using the visible and mid-infrared band (Xu, 2006) from Landsat imagery(Rokni*et al.*, 2014).

Surface water area

The MNDWI and JRC datasets were co-registered to each other. MNDWI was reclassified and then further extracted using the JRC dataset as a water mask. The MNDWI values were extracted for each image in the time series. The area statistics were derived from the reclassified MNDWI and calculated using ArcMap 10.8. The processed LULC and MNDWI were visualized on the maps to represent the changes in the surface water area spatially. MNDWI was validated using the surface water area extracted from the LULC, and a visual validation was performed using Google Earth.

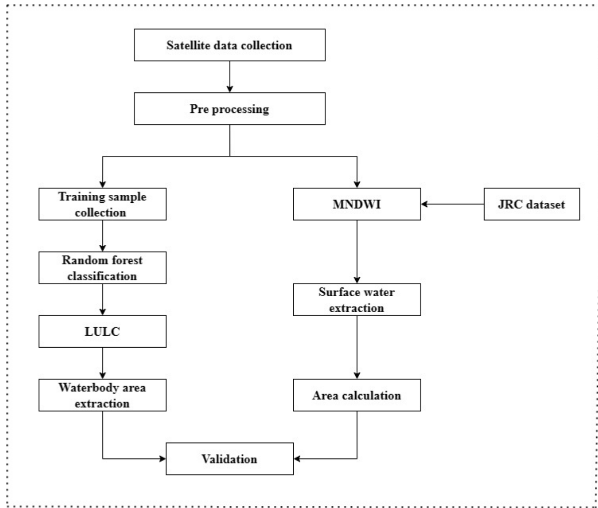

Fig. 2. Flowchart for evaluating the surface water change dynamics

MNDWI and calculated using ArcMap 10.8. The processed LULC and MNDWI were visualized on the maps to represent the changes in the surface water area spatially. MNDWI was validated using the surface water area extracted from the LULC, and a visual validation was performed using Google Earth.

The surface water area and the agricultural area were correlated for delineating the dependence of cultivated area during Rabi season on surface water resources.

Results and Discussion

Land use land cover change assessment

The year-wise LULC maps were generated at the GEE platform using the training sample collected over the regions. A Random Forest classification algorithm was used to classify the Landsat images during the Rabi cultivation season. The algorithm used 100 trees, and the samples were divided into training and testing sets in a 3:1 ratio. All the classified images achieved an overall accuracy of ~92%. The LULC map of the Bundelkhand region from 2013 to 2021 has been represented in Figure 3. The agricultural lands in the LULC maps represent the cultivated lands in the concerned growing period, i.e., the Rabi season. The rest of the cultivable agricultural lands are considered as the fallow lands. It was observed that the agricultural land area in the Rabi season increased by 26.24%, while the fallow land area decreased by 53.37% during 2013 to 2021 period.

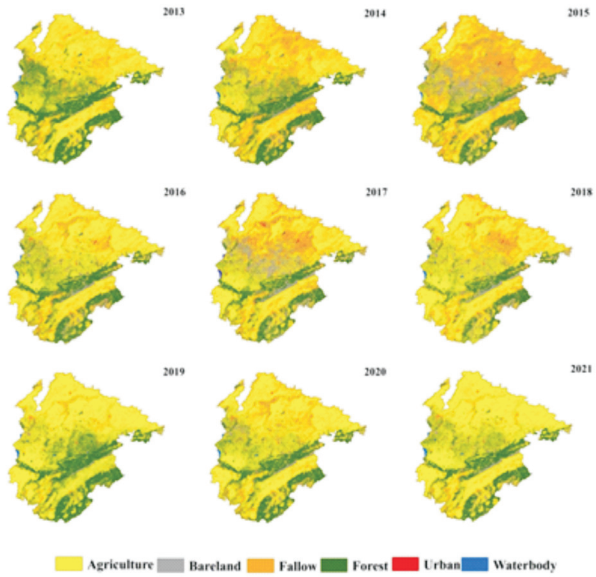

Fig. 3. Year-wise LULC map from 2013 to 2021 in the Rabi season

The agricultural lands showed a prominent increasing trend in the study area over time. However, from the LULC, the surface water dynamics fluctuated due to the uneven monsoon rainfall distribution over the area. The yearly distribution of the cropland and fallow land area in the Rabi season and the surface water area in the post-monsoon season has been mentioned in Table 2.

Assessment of MNDWI

Automatic extraction of the surface water using the MNDWI in the pre-and post-monsoon seasons was performed to understand the impact of rainfall variability and their relation to the agricultural expansion in the region. Figure 4 represents the MNDWI maps in the post-monsoon period from 2013 to 2021. The MNDWI values range from -1 to +1. Features with a value more than zero were considered water bodies and rests were classified into the non-water category. The surface water area extracted from the MNDWI images, when compared with that obtained from the LULC maps, showed an R^2 value of 0.88 (refer to Figure 5), indicating the robustness of the MNDWI for identifying water bodies. The maximum MNDWI value was observed in 2013 and the minimum in 2015.

Table 2. Year-wise distribution of cropland, fallow lands, and surface water area (hectares)

Year	Cropland	Fallow lands	Waterbody
2013	3858412	1163028	127503
2014	3402215	1710954	82951
2015	2447973	2148488	58431
2016	4199919	971612	99768
2017	3696396	1277371	69306
2018	4462401	1033319	91981
2019	4620467	552521	126702
2020	4385574	917179	90131
2021	4871174	542333	101949

Rainfall analysis

A declining trend in rainfall was observed from 2013

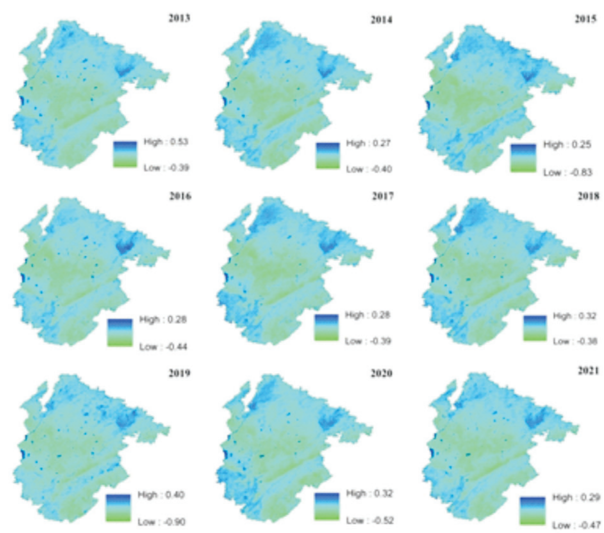

Fig. 4. Year-wise MNDWI maps showing the spatial distribution of the surface water area over time (2013-2021)

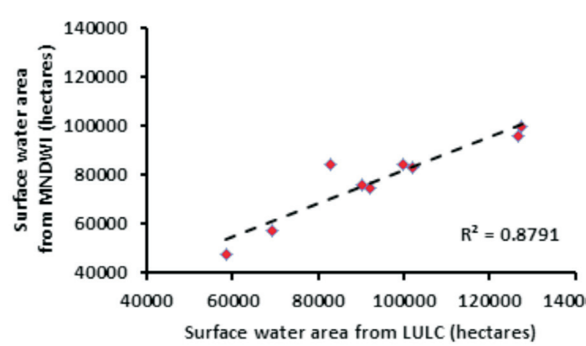

Fig. 5. Correlation between the surface water extracted from the LULC and the MNDWI

to 2021 (refer to Figure 6). The area received maximum monsoon rainfall in 2013 (1196 mm), followed by 2019 (944 mm). In 2013 and 2019, the area received about 31% and 6% excess rainfall compared to the normal. The minimum monsoon rainfall was observed in 2015 (493 mm). Significantly low rainfall caused about 48% rainfall deficiency in the region, resulting in lower MNDWI values, the minimum extent of Rabi cultivated lands, and the maximum extent of current fallow during the growing season. Figure 6 represents the distribution of the pre-and post-monsoon surface water area and the monsoon rainfall in the region over time.

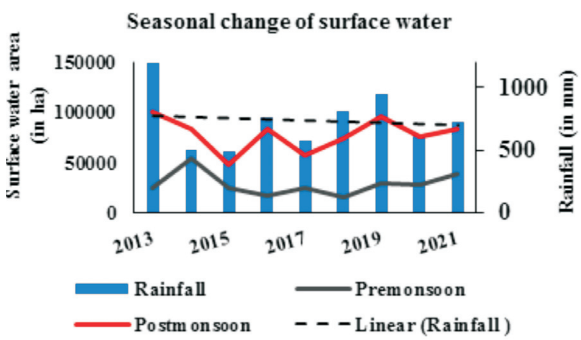

Fig. 6. Year-wise distribution of monsoon rainfall and the spatial extent of the surface water in the pre-and post-monsoon seasons

Relationship between surface water area and agricultural cropped area

Considering 2013 as the base year, a significant positive trend was observed in the increasing area converted to water bodies from cropland (refer to Figure 7). The expansion of existing water bodies and construction of new reservoirs in the study region eventually resulted in the encroachment of cropland and the subsequent increase in the surface water area. Figure 8 shows evidence of croplands being

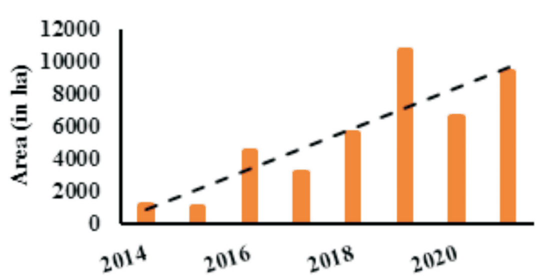

Fig. 7. Area converted to water body from cropland over time (2013-2014)

converted to water bodies by spatial expansion of the latter.

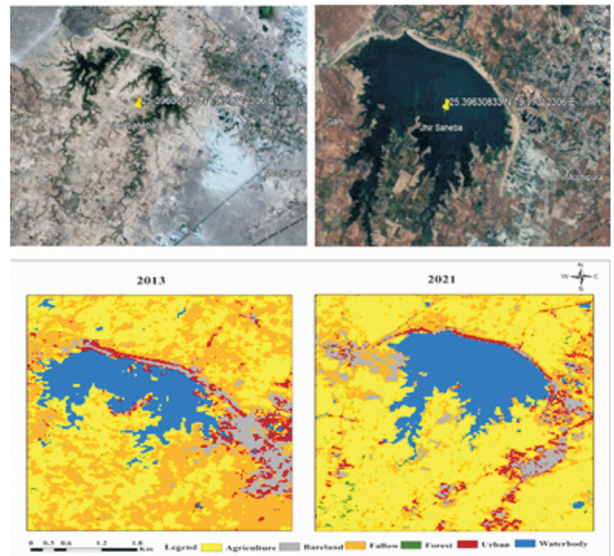

Fig. 8. Evidence of expansion of reservoir encroaching croplands over time; the high-resolution Google Earth images (above) and the LULC maps (below)

The surface water area expansion significantly helped to increase the cultivated land area, while decreased the fallow land area (Fig. 9). This indicated a significant dependent of cropped area on surface water availability.

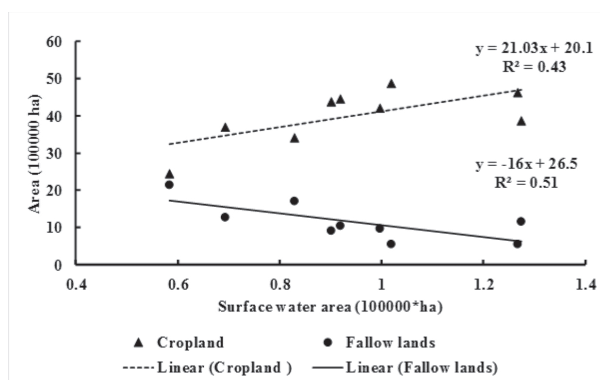

Fig. 9. Relationship between surface water area with cultivated and fallow area.

Discussion

Land use land cover change assessment has significant potential to extract the water bodies. However, misclassifying water pixels into the non-water classes, and vice-versa, might result in the lower accuracy of the concerned class. Hence, the MNDWI approach has been adopted in this study better to identify the water bodies in the study area. However, identifying the optimum threshold value is necessary to distinguish between the water and non-water features (Buma *et al.*, 2018). Qi *et al.* (2022) and Buma *et al.* (2018) mentioned that a threshold value of 0.2 is better for segmenting the water and non-water classes, as spectral information of the water bodies is maintained over this value. However, applying this threshold, some water pixels in our study area were misclassified into the non-water category. Hence, after testing with multiple threshold values, zero was confirmed, as suggested by Xu *et al.* (2006). Xu *et al.* (2006) also applied a threshold value of zero and obtained an overall accuracy of more than 95% for their study.

Spring wheat is the primarycrop grown in *Rabi* season in the study area. Cultivation of spring wheat requires an ample amount of irrigation water. Over time, the change detection analysis using the LULC showed an increasing trend for the area converted from cropland to the water body. Nevertheless, the expanded surface water area consequently improved irrigation practices in Bundelkhand, which resulted in the overall increase in cropped area and decrease in the fallow lands in Rabi season. The study highlights the need for increasing surface water area and water harvesting for overall improvement in agricultural area.

Conclusion

Satellite imageries with high spatial resolution like Landsat are very efficient for extracting earth surface features with better accuracy. The MNDWI method was proven to be a robust method for extracting the water bodies. This study evaluates the impact of water bodies' expansion on the existing agricultural system. The year-wise LULC analysis provided information about the increase in cropped area and decrease in fallow area with the increase of the surface water. It was observed that the agricultural area in Rabi season expanded by more than 25% from 2013 to 2021. On the other hand, the fallow area decreased by more than 50%, indicating a significant increase in the area under cultivation in the Rabi season. The outcomes of this study give an insight into the relationship between water availability and the existing cropping pattern, fulfilling the primary objective of the research. The increasing trends in the water area led to the expansion of the cultivated lands in the Rabi season. It was observed that 2015 received the least monsoon rainfall, resulting in minimum surface water area and the least cultivated area. However, the research provides further scope to evaluate the impact of improved irrigation practices on crop productivity in Bundelkhand.

Acknowledgement

The first author gratefully acknowledges the Indian Council of Agricultural Research (ICAR) – Indian Agricultural Research Institute for providing financial assistance for carrying out doctoral study.

Declarations

Conflicts of Interest: The authors declared thatthere are no competing or conflicting interests.

References

Acharya, T.D., Lee, D.H., Subedi, A. and Huang, H., 2019. Application of Water Indices in Surface Water Change Detection Using Landsat Imagery in Nepal. *Sensors & Materials.* 31.

Acharya, T.D., Subedi, A. and Lee, D.H., 2018. Evaluation of water indices for surface water extraction in a Landsat 8 scene of Nepal. *Sensors*. 18(8):2580.

Ahmed, A., Kumari, A., Singh, S.K. and Mondal, S. 2019. Rainfall variability assessment over Bundelkhand region and its impact on rainfed agriculture.

Arcgis, 2021. Indices gallery-arcgis Pro | Documentation. Available at: https://pro.arcgis.com/en/pro-app/latest/help/data/imagery/indices-gallery.htm#ESRI_SECTION1_4A9799E8F3E845 D8AFA6B9A3F467C5F9 (Accessed: 5 March 2021).

Buma, W.G., Lee, S.I. and Seo, J.Y. 2018. Recent surface water extent of Lake Chad from multispectral sensors and GRACE. *Sensors.* 18(7): 2082.

Domenikiotis, C., Loukas, A. and Dalezios, N.R. 2003. The use of NOAA/AVHRR satellite data for monitoring and assessment of forest fires and floods. *Natural Hazards and Earth System Sciences.* 3(1/2):115-128.

EOS landviewer 2021 *EOS landviewer: Find And Download Satellite Imagery*. Available at: https://eos.com/find-satellite/ (Accessed: 1 March 2021).

ESA (2021) *Sentinel-2 MSI - Level-2A Product - Sentinel Online - Sentinel Online*. Available at: https://sentinel.esa.int/web/sentinel/user-guides/sentinel-2-msi/product-types/level-2a (Accessed: 22 November 2021).

Feyisa, G.L., Meilby, H., Fensholt, R. and Proud, S.R. 2014. Automated Water Extraction Index: A new technique for surface water mapping using Landsat imagery. *Remote Sensing of Environment.* 140: 23-35.

Geographic, N. 2019. Surface Water | National Geographic Society. Available at: https://www.nationalgeographic.org/encyclopedia/surface-water/ (Accessed: 16 June 2021).

Google Earth Engine 2020. *USGS Landsat 7 Surface Reflectance Tier 1 | Earth Engine Data Catalog*, *USGS Landsat 7 Surface Reflectance Tier 1 | Earth Engine Data Catalog*. Available at: https://developers.google.com/earth-engine/datasets/catalog/LANDSAT_LE07_C01_T1_SR#description (Accessed: 17 June 2021).

Gorelick, N., Hancher, M., Dixon, M., Ilyushchenko, S., Thau, D. and Moore, R. 2017. Google Earth Engine: Planetary-scale geospatial analysis for everyone. *Remote sensing of Environment.* 202: 18-27.

Gupta, A. Kumar, 2014. *Bundelkhand Drought.* pp. 1–134.

Herndon, K. 2020. Assessment of surface water detection methods for water resource management in the Nigerien Sahel. *Sensors (Switzerland).* 20(2):1-14. Doi: 10.3390/s20020431.

Huang, C. 2018. Detecting, Extracting, and Monitoring Surface Water from Space using Optical Sensors: A Review. *Reviews of Geophysics.* 56(2):333–360. Doi: 10.1029/2018RG000598.

Ji, L., Zhang, L. and Wylie, B. 2009.Analysis of Dynamic Thresholds for the Normalized Difference Water Index. *Photogrammetric Engineering & Remote Sensing.* 75(11): 1307–1317. Doi: 10.14358/PERS.75.11.1307.

Krishnan, R. 2020. Assessment of climate change over the Indian region: A report of the ministry of earth sciences (MOES), government of India, Assessment of Climate Change over the Indian Region: A Report of the Ministry of Earth Sciences (moes), Government of India. Doi: 10.1007/978-981-15-4327-2.

Kumar, R., Singh, S.K. and Sah, U. 2017. Multidimensional study of pulse production in bundelkhand region of India. *Legume Research.* 40(6): 1046–1052. Doi: 10.18805/LR-3502.

Li, W. 2013.A Comparison of Land Surface Water Mapping Using the Normalized Difference Water Index from TM, ETM+ and ALI. *Remote Sensing.* 5(11): 5530–5549. Doi: 10.3390/rs5115530.

Magruder, O. 2019. What is an ID? A survey study. *Online Learning Journal.* 23(3): 137-160. Doi: 10.24059/olj.v23i3.1546.

Nie, W. 2011. Assessing impacts of Landuse and Landcover changes on hydrology for the upper San Pedro watershed. *Journal of Hydrology*. 407(1–4):105-114. Doi: 10.1016/j.jhydrol.2011.07.012.

Pai, D.S. 2014. Development of a new high spatial resolution (0.25° × 0.25°) long period (1901-2010) daily gridded rainfall data set over India and its comparison with existing data sets over the region. *Mausam*. 65(1): 1-18.

Pekel, J.F. 2016. High-resolution mapping of global surface water and its long-term changes. *Nature.* Nature Publishing Group. 540(7633): 418-422. Doi: 10.1038/nature20584.

Pekel, J.F. 2016. Global Surface Water Explorer, 2016. Available at: https://global-surface-water.appspot.com/#features (Accessed: 20 June 2021).

Pricope, N.G. 2013.Variable-source flood pulsing in a semi-arid transboundary watershed: The Chobe River, Botswana and Namibia. *Environmental Monitoring and Assessment.* 185(2):1883-1906. Doi: 10.1007/s10661-012-2675-0.

Qi, Y., Dou, H. and Wang, Z. 2022. March. An adaptive threshold selected method from remote sensing image based on water index. In *Journal of Physics: Conference Series.* 2228(1): 012001). IOP Publishing.

Rad, A.M., Kreitler, J. and Sadegh, M. 2021. Augmented Normalized Difference Water Index for improved surface water monitoring. *Environmental Modelling and Software.* Elsevier Ltd, 140, p. 105030. Doi: 10.1016/j.envsoft.2021.105030.

Rokni, K. 2014. Water Feature Extraction and Change Detection Using Multitemporal Landsat Imagery. *Remote Sensing.* 6(5): 4173-4189. Doi: 10.3390/rs6054173.

Tewari, R.K. 2018. Contingency Plan during Abnormal Weather for Bundelkhand Region. 003: 40.

Tulbure, M.G. 2016. Surface water extent dynamics from three decades of seasonally continuous Landsat time series at subcontinental scale in a semi-arid region. *Remote Sensing of Environment.* Elsevier Inc. 178:142-157. Doi: 10.1016/j.rse.2016.02.034.

Wang, X. 2020. Mapping coastal wetlands of China using time series Landsat images in 2018 and Google Earth Engine. *ISPRS Journal of Photogrammetry and Remote Sensing*. 163(March): 312-326. Doi: 10.1016/j.isprsjprs.2020.03.014.

Xu, H. 2006. Modification of normalized difference water index (NDWI) to enhance open water features in remotely sensed imagery. *International Journal of Remote Sensing.* 27(14): 3025-3033. Doi: 10.1080/01431160600589179.

Yang, X. 2017. Mapping of Urban Surface Water Bodies from Sentinel-2 MSI Imagery at 10 m Resolution via NDWI-Based Image Sharpening. *Remote Sensing.* 9(6): 596. Doi: 10.3390/rs9060596.